

The prognosis of extrahepatic and perihilar cholangiocarcinoma is very poor. The overall survival rate is less than 5% and curative surgical resection is just appropriate in about 20% of cases and associated with an overall 5-year survival of not more than 10-30% after curative resection in selected series [9-12]. This is due mainly to the fact that this cancer has an asymptomatic course of early stage and that diagnostic tools currently available are used too late or are not able to detect the early stages of disease [13]. PDT may play a curative or palliative role in the management of cholangiocarcinoma. Cholangiocarcinoma provides an ideal situation for interventions utilizing PDT with the possibility of curability for the commonly localized small tumors. As a palliative therapy, PDT has recently been shown to reduce cholestasis and improve quality of life in a small number of patients with Stage IV cholangiocarcinoma [14].

In the present study, we evaluated the anti-tumor effects of PDT using HMME as the photosensitizer and a 630 nm diode laser in human cholangiocarcinoma cell line QBC939.

Materials and methods

Photosensitizer. HMME hydrosolvent was purchased from HuaDing Bio-Pharmaceutical Co. (ChongQing, China). HMME solution was freshly prepared prior to use by dissolving in fetal calf serum (FCS)-free RPMI 1640 at a concentration of 10 mg/ml and kept in the dark at 4 °C. Further dilution of HMME was carried out in FCS-free RPMI 1640 to reach different concentrations.

Laser units. A diode laser (Diomed 630PDT Laser, United Kingdom) was used as the light source for exciting HMME. This diode laser is a continuous-wave laser operating at 630 nm wavelength.

Cell culture. Human cholangiocarcinoma cell line QBC939 was a kind gift from Dr Shuguang Wang (Third Military Medical University, Chongqing, China). QBC939 cells were maintained in a humidified 5% CO₂ incubator at 37 °C in RPMI 1640 (Gibco) supplemented with 10% FCS (Gibco), 100 IU/ml penicillin and 100 mg/ml streptomycin. All experiments were carried out in exponentially growing cells.

Photodynamic therapy and photocytotoxicity assay. QBC939 cells in 200 µl of 10% FCS RPMI 1640 medium (1.5×10^4 cells/well) were incubated in the 96-well flat-bottomed microtiter plates at 37 °C in a 5% CO₂ incubator. When cells were in exponential growth phase, the supernatants were removed and replaced with 200 µl fresh FCS-free medium. The cells were incubated with varying concentrations of HMME (0, 0.5, 1.0, 1.5, 2.0 µg/ml) for 3 h. The medium containing the drug was then aspirated and the cells were rinsed with phosphate buffered saline (PBS) and then replacing with another 200 µl RPMI 1640 before illumination. Irradiation was carried out at different light doses (0, 3, 9, 18, 27 J/cm²) at 630 nm with an output of 100 mW. Following this treatment, medium was replaced by 10% FCS RPMI 1640 and the cells were grown on again for a further 24 h. To evaluate cell viability and thus calculate the percentage of

phototoxicity, 3-(4,5-dimethylthiazol-2-yl)-2,5-diphenyltetrazolium bromide (MTT) assay was employed. Briefly, the cells with media only served as a positive control and 200 µl of the medium alone without cells and reagent was used as a negative control. Following photodynamic treatment of the cells in microtiter plates as mentioned above, 20 µl of the MTT dye (5 mg/ml, Sigma) was added into each well. The unreactive supernatants in the well were carefully aspirated and replaced with 100 µl of isopropanol supplemented with 0.05 M HCl to solubilize the reactive dye. The absorbance (A) values of each well at 540 nm were read using an automatic multiwell spectrophotometer (Bio-Rad, Japan). The negative control well was used for zeroing absorbance. The percentage of cytotoxicity was calculated using the background-corrected absorbance as follows:

$$\text{inhibitive rate} = (1 - [A \text{ of experimental well}/A \text{ of positive control well}]) \times 100\%$$

Experiments were performed at least three times with representative data presented.

Determination of cell death and apoptosis or necrosis image detection. Apoptosis or necrosis detection post-PDT were determined by flow cytometer using the Annexin V-FITC Apoptosis Kit (BD Bioscience, USA). Approximately 1×10^6 QBC939 cells that had received photodynamic treatment (HMME 0.5, 1.5 µg/mL, light dose 3, 9 J/cm², 3 h after incubation) were gently scraped and washed twice with cold PBS at 8 h following photodynamic treatment. Cells were resuspended with 100 µl annexin-V binding buffer then incubated with 10 µl annexin-V for 15 min at room temperature in the dark. Then 400 µl binding buffer containing 5 µl PI was added to the cells and incubated on ice for 15 min. The cells were sampled with a FACS Calibur flow cytometer (Becton Dickinson, USA) within 1 h. A total of 1×10^4 cells were analyzed in each sample. Data analysis was carried out with CELLQuest software (Becton Dickinson, USA). The results were interpreted as Table. 1.

Table. 1 Explanation for results of flow cytometer

Quadrant	Meaning
I. Lower left quadrant	annexin V(-)/PI(-): considered as living cells
II. Lower right quadrant	annexin V(+)/PI(-): considered as apoptotic cells
III. Upper right quadrant	annexin V(+)/PI(+): considered as necrotic cells
IV. Upper left quadrant	annexin V(-)/PI(+): considered as bare nuclei, cells in late necrosis, or cellular debris.

QBC939 cells were incubated in 12-well flat-bottomed microtiter plates. Three hours after HMME was added, the cells received photodynamic treatment (HMME 1.0 µg/ml, light dose 3 J/cm²) as described above. The cell samples were rinsed with fresh medium and stained with the Annexin V-FITC Apoptosis Kit (BD Bioscience, USA) at 8 and 16

h after irradiation. All images were then captured using the laser scanning confocal microscope (LSCM, Zeiss 510 meta, Germany) to assess the staining differences of apoptosis or necrosis. The results were interpreted as follows: cells display green fluorescence as apoptotic cells; cells display red fluorescence as late necrosis cells; cells display green and red fluorescence as necrosis cells.

TUNEL assay. TUNEL assay was performed using the DNA Fragmentation Detection Kit (Roche, Germany). We selected QBC939 cells in logarithmic growth phase, and using inoculated culture dishes placed with 6×6 mm coverslips. Then coverslips were incubated with HMME for 3 h, the cells received photodynamic treatment (HMME $1 \mu\text{g/ml}$, light dose 18 J/cm^2) as described above. Air dried cell samples were fixed with paraformaldehyde solution for 30 min at 8 h after irradiation. Coverslips were rinsed with PBS and incubated with blocking solution (0.3% H_2O_2 in methanol) for 30 min. Coverslips were rinsed with PBS and incubated in permeabilisation solution (0.1% Triton X-100 in 0.1% sodium citrate) for 2 min in ice. TUNEL reaction mixture were added with $50 \mu\text{l}$ in sample. Coverslips were incubated in a humidified chamber for 1 h at 37°C . Coverter-POD were added with $50 \mu\text{l}$ in sample. Coverslips were incubate in a humidified chamber for 30 min at 37°C . Coverslips were rinsed with PBS for three times. DAB substate solution were added with $50\text{--}100 \mu\text{l}$ for 15 min. Coverslips were rinsd with PBS for three times and were mountd above glass slides, then analysed under light microscope.

Western blot analysis. After the QBC939 cells received photodynamic treatment (HMME 1, 2 $\mu\text{g/ml}$, light dose 9, 27 J/cm^2) as described above. Cell pellets were washed once with ice-cold PBS and lysed in lysis buffer (20 mM HEPES-KOH, 250 mM sucrose, pH 7.5, 10 mM KCl, 1.5 mM MgCl_2 , 1 mM sodium EDTA, 1 mM dithiothreitol and 0.1 mM phenylmethylsulfonyl fluoride) at 8 h. The cells were homogenized on ice for 15 min and the homogenates were centrifuged twice at 1000 g for 10 min. The supernatants were centrifuged at $12,000 \text{ g}$ for 15 min at 4°C , and the resulting supernatants were cytosol without mitochondria. The protein concentration of cell extracts was determined using a Bradford protein assay. Cytosol protein was loaded and separated on 12% sodium dodecyl sulfate (SDS) polyacrylamide gel and transferred to a nitrocellulose membrane by standard electric transfer protocol. The membranes were blocked with 0.5% dry milk in PBS. The primary antibodies used were mouse antihuman cytochrome C and caspase-3 monoclonal antibody (1 : 3000, Santa, USA), and the secondary antibody was horseradish peroxidase-conjugated goat anti-mouse IgG (1 : 5000, Santa, USA). The membranes were hybridized according to the Amersham's ECL protocol. The membrane was exposed to X-ray film. The relative level of cytochrome C and caspase-3 was obtained after normalization with the level of β -actin in the same lane.

Statistical analysis. All data were presented as mean \pm SD of three independent experiments. Statistical significance was determined using Student's *t*-test. $P < 0.05$ was considered statistically significant.

Results

Photocytotoxicity assay. Fig. 2 shows the inhibitive rate curve. MTT assay showed that there was no significant difference in the survival rate of cells exposed to light alone ($P > 0.05$) or HMME alone ($P > 0.05$) compared to blank controls (neither light nor HMME). HMME alone or laser alone showed no cytotoxicity to QBC939 cells, which was important because it indicated that no dark toxicity existed concerning HMME. When HMME combined with laser illumination, the photocytotoxicity were both drug dose- and light dose-dependent. The inhibitive rate of cells was significantly increased with increasing light dose ($0\text{--}27 \text{ J/cm}^2$, $P = 0.004$). The same difference was observed with an increasing HMME dose ($0\text{--}2.0 \mu\text{g/ml}$, $P = 0.002$). QBC939 cells seemed very sensitive to HMMEbased PDT. When the HMME dose reached $2.0 \mu\text{g/ml}$, lots of cells were killed even in a lower laser dose (3 J/cm^2).

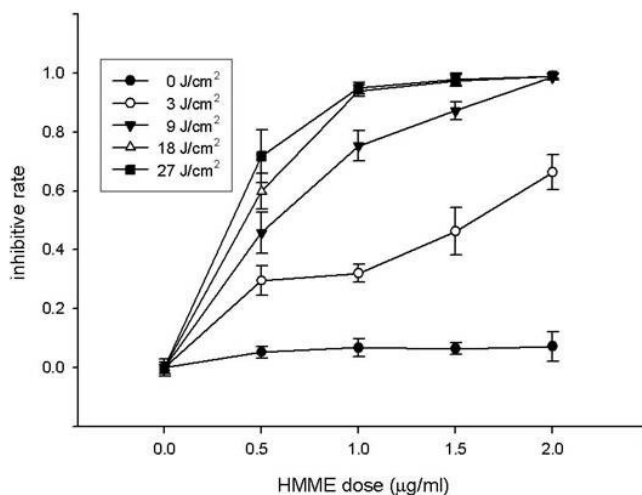


Figure 2 Photocytotoxicity of hematoporphyrin monomethyl ether (HMME) to QBC939 cells. Shown are the cell inhibitive rates at 24 h after photodynamic treatment with different concentrations of HMME (0–2.0 $\mu\text{g/ml}$) and different light doses (0–27 J/cm^2).

Flow cytometric analysis and apoptosis or necrosis image

PI uptake by At 8 h following PDT, dual staining of cells with Annexin V/PI and analysis using flow cytometry were used to distinguish apoptotic from necrotic cells. Flow cytometry dot plots of the simultaneous binding of Annexin V–FITC and cells are shown in Fig. 3. The apoptotic cells were mainly characterized as Annexin V(+)/PI(–), representing apoptosis. Therefore, HMME-based PDT induced direct apoptosis rather than necrosis in QBC939 cells.

Fig. 4(a) shows strong green fluorescence of QBC939 cells at 8 h after photodynamic treatment indicating apoptotic cells, the membrane of cells were intact. Fig. 4(b) shows weaker green fluorescence in the cellular membrane and red fluorescence in the cellular nucleus at 16 h following PDT, which indicated cellular membrane disrupted. The cells had transition from apoptosis to necrosis.

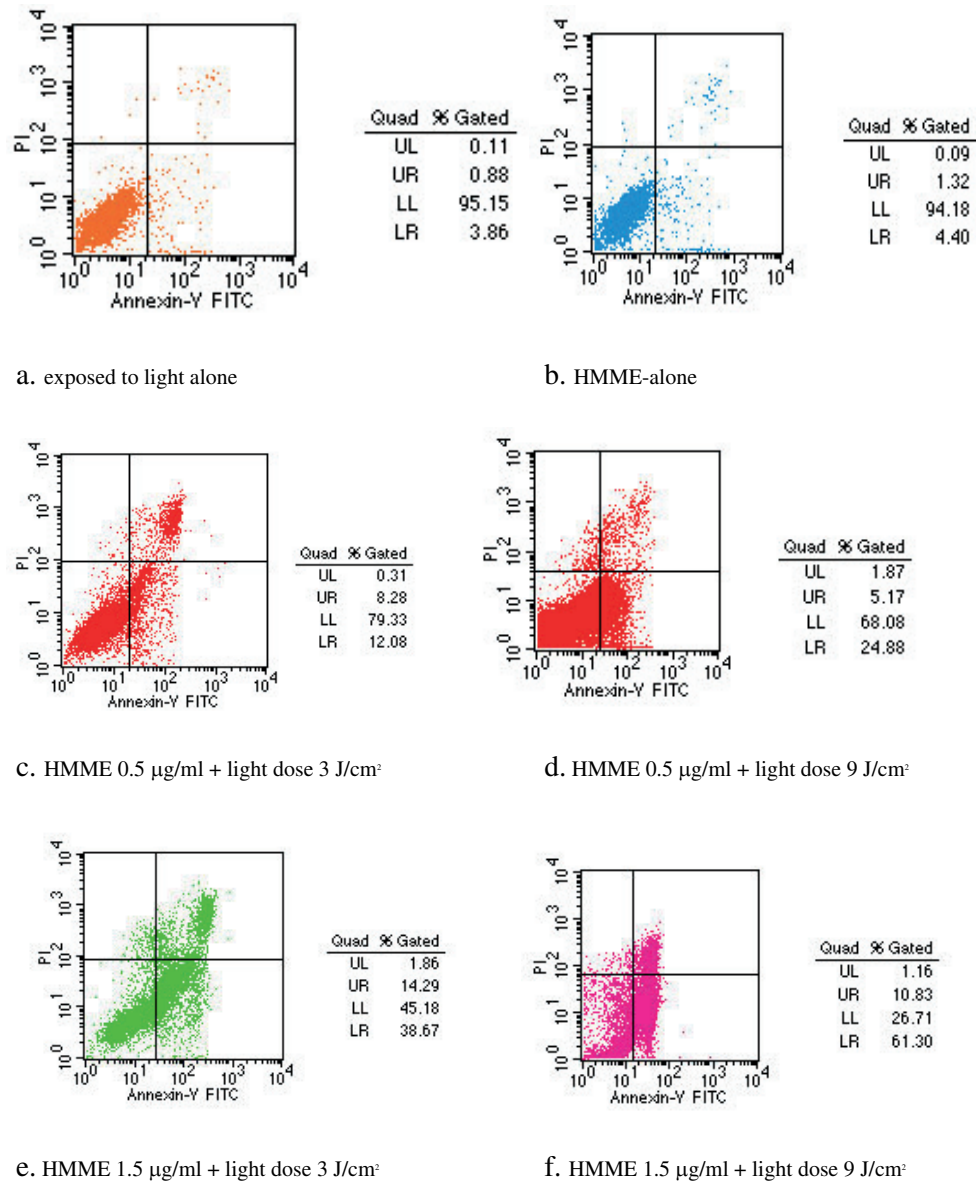


Figure 3 Cell death mode induced by hematoporphyrin monomethyl ether-based photodynamic treatment. Flow cytometry analysis of QBC939 cells.

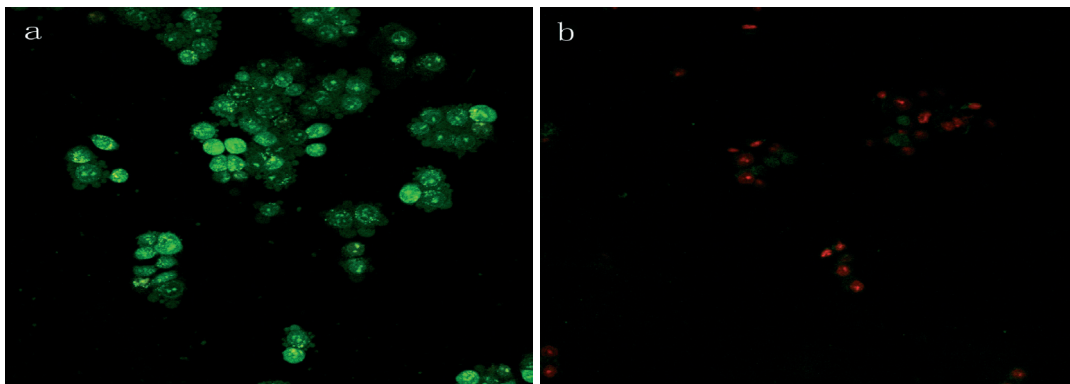


Figure 4 LSCM image of QBC939 cell after PDT.

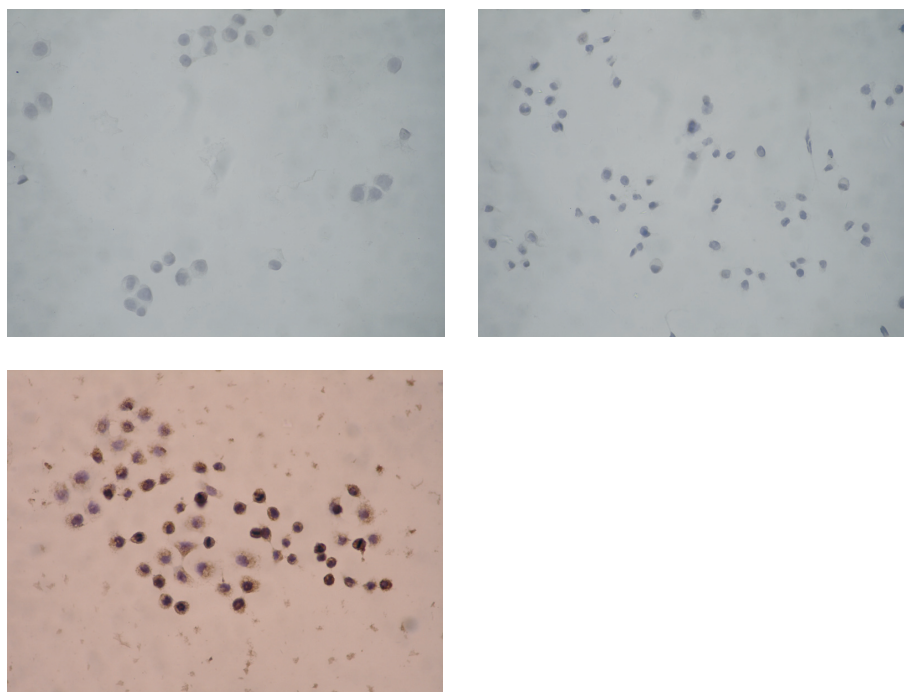


Figure. 5 TUNEL assay of QBC939 cells after PDT. a. HMME-alone b. exposed to light alone c. HMME 1 µg/ml + light dose 18 J/cm²

TUNEL assay. Fig. 5 shows QBC939 cells treated with PDT were assayed for apoptosis by TUNEL. QBC939 cells could induce apoptosis. The abnormal chromatin clumps, nuclear membrane wrinkling, nuclear collapse, cytoplasm bubble and cytomembrane wrinkling had appeared after treatment with PDT. Apoptotic cells were not shown by TUNEL assay in HMME-alone and exposed to light alone cells. In this kit terminal deoxynucleotidyl transferase, which catalyzes polymerization of nucleotides to free 3'-OH DNA ends in a template-independent manner, was used to label DNA strand

breaks. After substrate reaction, stained cells can be analyzed under light microscope.

Assay for cytochrome and procaspase-3. The Western blot analysis indicated the release of cytochrome c from the mitochondria into cytosol after PDT (Fig. 6a). Increased levels of cytochrome c were notably detected in the cytosol after 8 h. To determine whether caspase-3 plays a role in berbamine mediated apoptosis of QBC939 cells, we assessed the procaspase-3 protein level of the QBC939 cells before and after treatment with PDT. Western blot result showed that procaspase-3 decreased (Fig. 6b).

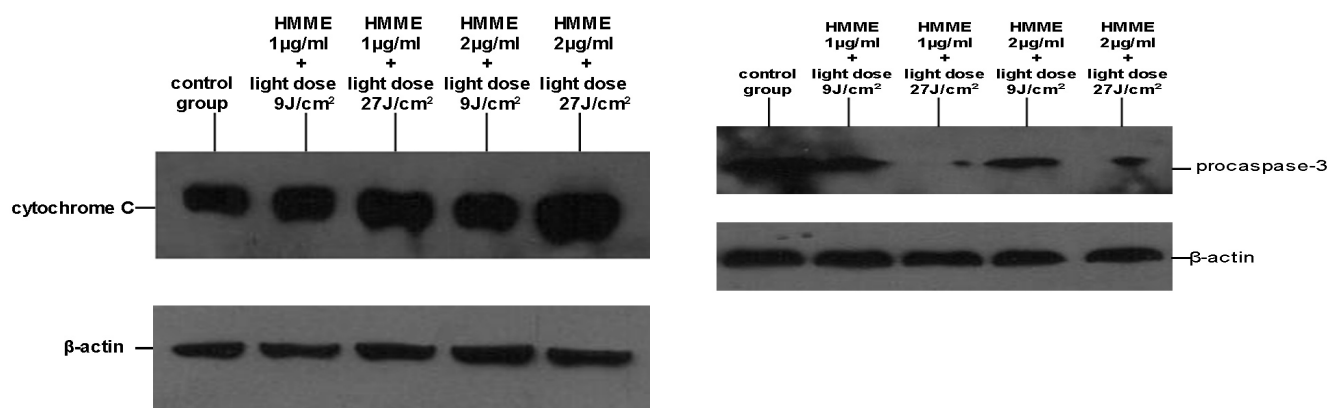


Figure. 6

Discussion

The poor prognosis of cholangiocarcinoma and recent development in photomedicine have generated a considerable interest in PDT for this disease. Wong Kee Song et al have successfully treated cholangiocarcinoma nodules on the peritoneal surface with laser-light activated mono-l-aspartyl chlorin e6 (NPe6) and HpD in nude mice, resulting in prolongation of survival [15]. Clinical studies also showed favorable results of photodynamic therapy for cholangiocarcinoma patients [16–18]. HMME is a novel second generation of photosensitizers, we provided the evidences that HMME is a novel photosensitizer for cholangiocarcinoma treatment.

The cytotoxic efficacy of PDT relies on a bimodal protocol comprised of a chemical photosensitizer and light irradiation. Neither the photosensitizer nor the light alone is toxic [19]. Our study shows that no apoptotic phenomena were observed in QBC939 cells treated either with a photosensitizer only or light only. However, these two elements in combination induced apoptosis in QBC939 cells, which are particularly resistant to cell death via apoptosis, irrespective of the stimuli. The results are consistent with the conclusion mentioned above.

In addition to the development of new photosensitizers, continued improvements in clinical PDT will come from the translation of information generated from studies examining basic mechanisms of this procedure. Apoptotic and necrotic pathways are both involved in PDT mediated cell death [20]. To determine the underlying mechanisms of the growth inhibitory effect of PDT, we investigated whether PDT using HMME act by inducing apoptosis of human cholangiocarcinoma cells. For this purpose, we performed TUNEL assays and LSCM for the detection of fragmented mono and oligo-nucleosomes. In both assays, apoptosis was observed in human cholangiocarcinoma cell lines that were treated with HMME and diode laser.

PDT can induce cell death through necrosis or apoptosis both in vivo and in vitro, the type of cell death triggered by PDT is dependent on the photosensitizer used, illumination conditions, oxygenation status of tissue, and the type of cells involved [21]. As shown in Fig. 3, two types of cell death, apoptosis and necrosis were observed in the QBC939 cells receiving HMME-PDT as performed in this study, but apoptosis preferentially occurred. Mitochondria play a pivotal role in apoptosis, the release of cytochrome c from mitochondria into the cytosol triggers the assembly of Apaf-1 (apoptotic protease-activating factor) and procaspase-9 to form an apoptosome in the presence of dATP or ATP. Procaspase-9 is then autocleaved to active caspase-9, which in turn activates procaspase-3 to active caspase-3, resulting in cleavage of its substrates and apoptosis. Our study provides PDT using HMME increased considerably the release of cytochrome c from mitochondria at an early stage in QBC939 cells and decreased the content of procaspase-3. Results from our study demonstrated that treatment of the human cholangiocarcinoma cells with PDT initiates early cytochrome c release, followed by late caspase activation.

PDT may be of importance in the treatment of human cholangiocarcinoma. The tumor is usually localized but often unresectable due to involvement of critical structures, such as bifurcation of the common bile duct. Localized therapy can be applied to such lesions using endoscopically placed fibers that can easily traverse almost all stenotic lesions. This therapy would be considered minimally invasive and produce minimal systemic toxicity [22]. The role of PDT may not only be palliative in terms of improving bile flow but conceivably even curative in the treatment of early lesions, as has been found for patients with predisposing conditions such as primary sclerosing cholangitis.

In conclusion, the present study demonstrates that PDT using HMME and the 630nm laser induces cell death, mainly through apoptosis in human cholangiocarcinoma cells. From our studies, the mechanism of apoptosis induced PDT using HMME appears to involve release of cytochrome c into the cytoplasm and caspase activation. Although further studies are needed for the technical aspect, it is expected that this therapy, after finalizing experimental studies, could be clinically useful for the treatment of patients with cholangiocarcinoma.

Acknowledgements. This study was supported by the New Century Talents Supporting Scheme (NCET-06-0350), China.

References

- [1] IGARASHI A, KONNO H, TANAKA T, NAKAMURA S, SADZUKA Y, et al. Liposomal photofrin enhances therapeutic efficacy of photodynamic therapy against the human gastric cancer. *Toxicol Lett* 2003; 145: 133–141. doi:10.1016/S0378-4274(03)00241-8
- [2] LIPSON RL, BALDES EJ, OLSEN AM. The use of a derivative of hematoporphyrin in tumor detection. *J Natl Cancer Inst* 1961; 26: 1–11.
- [3] SHARMAN WM, ALLEN CM, VAN LIER JE. Photodynamic therapeutics: basic principles and clinical applications. *Drug Discov Today*. 1999; 4: 507–517. doi:10.1016/S1359-6446(99)01412-9
- [4] SVAASAND LO. Optical dosimetry for direct and interstitial photoradiation therapy of malignant tumors. *Prog Clin Biol Res*. 1984; 170: 91–114.
- [5] DOUGHERTY TJ. An update on photodynamic therapy applications. *J Clin Laser Med Surg*. 2002; 20: 3–7. doi:10.1089/104454702753474931
- [6] CARRUTH JA. Clinical applications of photodynamic therapy. *Int J Clin Pract*. 1998; 52: 39–42.
- [7] ZHENG H. Photodynamic therapy in China: over 25 years of unique clinical experience. Part one – history and domestic photosensitizers. *Photodiag Photodynamic Ther*. 2006; 3: 3–10. doi:10.1016/S1572-1000(06)00009-3
- [8] XU DY. Research and development of photodynamic therapy photosensitizers in China. *Photodiag Photodynamic Ther*. 2007; 4: 13–25. doi:10.1016/j.pdpdt.2006.09.003
- [9] AYARU L, BOWN SG, PEREIRA SP. Photodynamic therapy for pancreatic and biliary tract carcinoma. *Int J Gastrointest Cancer*. 2005; 35: 1–13. doi:10.1385/IJGC:35:1:001

- [10] LAZARIDIS KN, GORES GJ. Cholangiocarcinoma. *Gastroenterology*. 2005; 128: 1655–1667. [doi:10.1053/j.gastro.2005.03.040](https://doi.org/10.1053/j.gastro.2005.03.040)
- [11] DE GROEN PC, GORES GJ, LARUSSO NF, GUNDERSON LL, NAGORNEY DM. Biliary tract cancers. *N Engl J Med*. 1999; 341: 1368–1378. [doi:10.1056/NEJM199910283411807](https://doi.org/10.1056/NEJM199910283411807)
- [12] LEONARD GD, O'REILLY EM. Biliary tract cancers: current concepts and controversies. *Expert Opin Pharmacother*. 2005; 6: 211–223. [doi:10.1517/14656566.6.2.211](https://doi.org/10.1517/14656566.6.2.211)
- [13] WANG JB, LIU LX. Use of photodynamic therapy in malignant lesions of stomach, bile duct, pancreas, colon and rectum. *Hepatogastroenterology*. 2007; 54: 718–724.
- [14] ORTNER MA, DORTA G. Technology insight: Photodynamic therapy for cholangiocarcinoma. *Nat Clin Pract Gastroenterol Hepatol*. 2006; 3: 459–467. [doi:10.1038/ncpgasthep0543](https://doi.org/10.1038/ncpgasthep0543)
- [15] WONG KEE SONG LM, WANG KK, ZINSMEISTER AR. Mono-L-aspartyl chlorin e6 (NPe6) and hematoporphyrin derivative (HpD) in photodynamic therapy administered to a human cholangio-carcinoma model. *Cancer*. 1998; 82: 421–427. [doi:10.1002/1097-0142\(19980115\)82:2<421::AID-CNCR25>3.0.CO;2-O](https://doi.org/10.1002/1097-0142(19980115)82:2<421::AID-CNCR25>3.0.CO;2-O)
- [16] RUMALLA A, BARON TH, WANG KK, GORES GJ, STADHEIM LM, et al. Endoscopic application of photodynamic therapy for cholangiocarcinoma. *Gastrointest Endosc*. 2001; 53: 500–504. [doi:10.1067/mge.2001.113386](https://doi.org/10.1067/mge.2001.113386)
- [17] ORTNER MA. Photodynamic therapy of cholangiocarcinoma cancer. *Gastrointest Endosc Clin N Am*. 2000; 10: 481–486.
- [18] ORTNER ME, CACA K, BERR F, LIEBETRUTH J, MANS-MANN U, et al. Successful photodynamic therapy for nonresectable cholangiocarcinoma: a randomized prospective study. *Gastroenterology*. 2003; 125: 1355–1363. [doi:10.1016/j.gastro.2003.07.015](https://doi.org/10.1016/j.gastro.2003.07.015)
- [19] CASAS A, FUKUDA H, DI VENOSA G, BATLLE A. Photosensitization and mechanism of cytotoxicity induced by the use of ALA derivatives in photodynamic therapy. *Br J Cancer*. 2001; 85: 279–284. [doi:10.1054/bjoc.2001.1875](https://doi.org/10.1054/bjoc.2001.1875)
- [20] WOODBURN KW, FAN Q, MILES DR, KESSEL D, LUO Y, et al. Localization and efficacy analysis of the phototherapeutic lutetium texaphyrin (PCI-0123) in the murine EMT6 sarcoma model. *Photochem Photobiol*. 1997; 65: 410–415. [doi:10.1111/j.1751-1097.1997.tb08579.x](https://doi.org/10.1111/j.1751-1097.1997.tb08579.x)
- [21] WYLD L, REED MW, BROWN NJ. Differential cell death response to photodynamic therapy is dependent on dose and cell type, *Br. J. Cancer*. 2001; 84: 1384–1386. [doi:10.1054/bjoc.2001.1795](https://doi.org/10.1054/bjoc.2001.1795)
- [22] ORTNER M. Photodynamic therapy for cholangiocarcinoma. *J Hepatobiliary Pancreat Surg*. 2001; 8: 137–139. [doi:10.1007/s005340170036](https://doi.org/10.1007/s005340170036)